

Seismic protection of base isolated structures using smart passive control system

Hyung-Jo Jung[†] and Kang-Min Choi[‡]

Department of Civil and Environmental Engineering, KAIST, Daejeon 305-701, Korea

Kyu-Sik Park[‡]

Department of Civil and Environmental Engineering, University of Illinois at Urbana Champaign, IL 61801, USA

Sang-Won Cho[‡]

The Boundary Layer Wind Tunnel Lab., The University of Western Ontario, Ontario, Canada

(Received October 31, 2006, Accepted December 28, 2006)

Abstract. The effectiveness of the newly developed smart passive control system employing a magnetorheological (MR) damper and an electromagnetic induction (EMI) part for seismic protection of base isolated structures is numerically investigated. An EMI part in the system consists of a permanent magnet and a coil, which changes the kinetic energy of the deformation of an MR damper into the electric energy (i.e. the induced current) according to the Faraday's law of electromagnetic induction. In the smart passive control system, the damping characteristics of an MR damper are varied with the current input generated from an EMI part. Hence, it does not need any control system consisting of sensors, a controller and an external power source. This makes the system much simpler as well as more economic. To verify the efficacy of the smart passive control system, a series of numerical simulations are carried out by considering the benchmark base isolated structure control problems. The numerical simulation results show that the smart passive control system has the comparable control performance to the conventional MR damper-based semiactive control system. Therefore, the smart passive control system could be considered as one of the promising control devices for seismic protection of seismically excited base isolated structures.

Keywords: MR damper; electromagnetic induction; smart passive control; base isolation system; seismic protection.

1. Introduction

A base isolation system is the most widely used seismic protection method for civil structures such as buildings and highway bridges (Skinner, *et al.* 1993). This system usually decouples the superstructure of a structure from its foundations or piers/abutments during earthquakes, resulting in significant reduction of the seismic forces induced in the structure as well as the strength and ductility demands on the structure. If a base isolation system is introduced to a building or a bridge, the responses of inter-

[†]Assistant Professor, Corresponding author, E-mail: hjung@kaist.ac.kr

[‡]Postdoctoral Fellow

story drifts and floor accelerations in the building or base shears and overturning moments in the bridge can be significantly reduced, respectively. On the other hand, the base displacements in buildings or the girder displacements in bridges may be slightly increased, particularly during near-field ground motions. It causes the expensive loss of space for the seismic gap.

The excessive displacement due to base isolators can be reduced by additional damping devices such as passive-type viscous dampers, however, it increases the responses in the piers such as base shears in bridges or inter-story drifts in buildings. In recent years, considerable attention has been paid to hybrid-type base isolation systems (i.e. the combination with passive-type base isolators and active- or semiactive-type additional control devices) as attractive alternatives. It is noted that hybrid-type control systems alleviate some of the limitations that exist for either a passive or active control system acting alone, thus leading to an improved solution. In particular, semiactive-type magnetorheological (MR) dampers are considered as one of the most promising additional devices for hybrid base isolation systems because of their mechanical simplicity, large force capacity, high dynamic range, low operation power requirement such as a battery, and environmental robustness (Kamath and Wereley 1997, Dyke and Spencer 1996, Spencer, *et al.* 1997).

Several hybrid-type base isolation systems employing additional active control devices have been analytically and experimentally studied with the goal of supplementing passive-type base isolation with active devices to limit base drift of the structure (Yang, *et al.* 1996, Ramallo, *et al.* 2002, Jung, *et al.* 2006, Lee, *et al.* 2006). Active control devices, however, have yet to be fully embraced by engineers, in large part due to the challenges of large power supplies, concerns about stability, and so on. Because semiactive control devices such as MR dampers have the potential to achieve the majority of the performance of fully active systems as well as offer the adaptability of active devices without requiring the associated large power sources, it is expected that the hybrid-type base isolation system employing additional semiactive control devices could solve the large base drift problem of the passive-type base isolation.

A conventional semiactive control strategy based on MR dampers needs a feedback control system consisting of a controller, sensors, and a power supply. Thus, a semiactive system is usually relatively expensive compared to a passive system. In addition, it is not easy to build up and maintain an MR damper-based semiactive control system for large-scale structures such as high-rise buildings and long-span bridges. To resolve the above difficulties, a smart passive control system that consists of an MR damper and an electromagnetic induction (EMI) part was proposed by Cho, *et al.* (2005). In the smart passive system, the damping characteristics of a damper can be changed by the EMI part consisting of permanent magnet and coil according to Faraday's law of electromagnetic induction. They numerically verified the effectiveness of the smart passive system by comparing its control performance with the normal MR fluid damper-based semiactive control system.

In this study, the effectiveness of the smart passive system based on MR dampers for seismic protection of base isolated civil structures such as buildings and highway bridges is investigated. To systematically verify its effectiveness, the benchmark structural control problems for a seismically excited highway bridge developed by Agrawal, *et al.* (2005) as well as a base isolated building developed by Narasimhan, *et al.* (2006) are examined. These benchmark studies are basically carried out based on input from the ASCE structural control committee. The base isolated building and bridge structures considered are an eight-story frame building with steel-braces and a continuous two-span concrete box-girder bridge, respectively. A series of numerical simulations are carried out, and the results of the smart passive system are compared with those of the conventional MR damper-based semiactive system.

2. Smart passive control system

In this section, the smart passive control system based on an MR damper used as a supplemental control system for improving the performance of a base isolation system is explained. A conventional semiactive control system using MR dampers needs a feedback control system. In other words, it requires sensors to measure the structural responses, a controller to calculate the required control command, and an external power source such as a battery to change the damping characteristics of MR fluids. Fig. 1 shows the schematic diagram of the conventional semiactive control system using an MR damper. As seen from the figure, the conventional system needs a feedback control system. Although it seems to be simple, the control system becomes more complicated to build up and maintain when many MR fluid dampers are used for large-scale civil engineering structures such as cable-stayed bridges and high-rise buildings.

On the other hand, the smart passive control system adopts an EMI part to replace a feedback control system (Cho, *et al.* 2005). An EMI part consists of a permanent magnet and a coil. Fig. 2 shows the schematic diagram of the smart passive system consisting of an MR damper and an EMI part.

An EMI part changes the kinetic energy of the reciprocation motion of an MR damper to the electric energy (i.e. induced current) according to the Faraday’s law of electromagnetic induction (Reitz, *et al.* 1993, Marshall and Skitek 1990, Miner 1996), and then the electric energy is used to change the damping characteristics of an MR damper by forming magnetic field in the damper. Thus, sensors, a controller, and an external power source are not needed in the smart passive system at all. The induced current according to the Faraday’s law of electromagnetic induction can be estimated as follows:

$$\varepsilon = -N \frac{d\Phi_B}{dt} = -N \cdot B \frac{dA}{dt} = -N \cdot B \cdot w \frac{dx}{dt} = -K_{emf} \frac{dx}{dt} \tag{1}$$

where is induced electromotive force (*emf*) (Volt), N is the number of turns of coil, Φ_B is magnetic flux

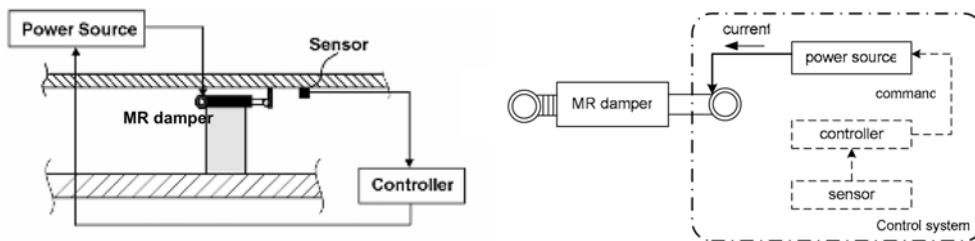


Fig. 1 Schematic of conventional MR damper-based semiactive control system

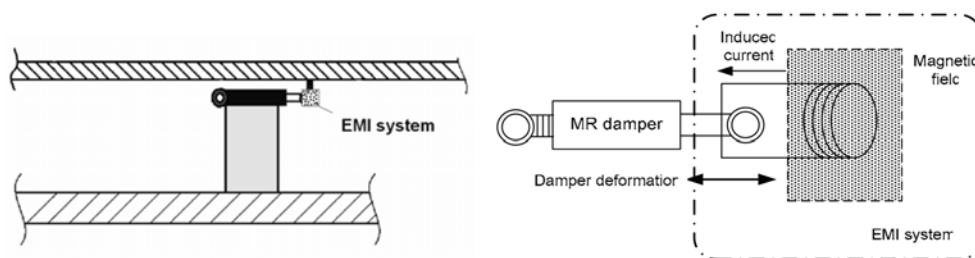


Fig. 2 Schematic of smart passive control system employing MR damper and EMI part

(Weber), B is the magnet field (Tesla), A is the area of the cross section (m^2), w is the width of magnet (m), and K_{emf} is the gain of the EMI part (Volt-sec/m). Negative sign in Eq. (1) is the direction of induced current.

Eq. (1) states that the relative motion between a coil and a permanent magnet causes a change in the magnet flux, which induces an *emf* in the coil. The amount of the induced *emf* can be regulated by the turns of the coil or the intensity of the permanent magnet as in Eq. (1). This induced the electric energy in the MR damper is used to make magnet fields that solidify the MR fluid inside the damper, which results in a change in damping characteristics of the MR damper. According to Eq. (1), hence, the fast relative motion of the MR damper induces the high current; the slow motion induces the low current from the EMI part.

Thus, an MR damper with an EMI part is capable of being adjusted to the vibration of structures by itself without any controller, power supply and sensors, because the output of the induced electric energy is proportional to the magnitude of input loads such as earthquakes. Hence, an MR damper-based smart control system including an EMI part has the adaptability that other passive control systems cannot have. This is one of the main attractive features of an EMI part in the smart passive control system. More detailed information on the EMI system can be found in Cho, *et al.* (2005).

3. Numerical examples

To systematically verify the effectiveness of the smart passive control system for base isolated structures, the two typical examples are considered as follows: Example 1; a base isolated building model and Example 2; a base isolated highway bridge model. Each structural model has been developed for the benchmark structural control problem by Narasimhan, *et al.* (2006) and Agrawal, *et al.* (2005), respectively. These benchmark studies have been carried out based on input from the ASCE structural control committee. The base isolated building and bridge structures considered are an eight-story frame building with steel-braces and a continuous two-span concrete box-girder bridge, respectively. A series of numerical simulations are carried out, and the results of the smart passive system are compared with those of the conventional MR damper-based semiactive system.

3.1. Example 1: base isolated building structure

3.1.1. Structural model

The benchmark structure is an eight-story frame building with steel-braces. Stories one to six have an L-shaped plan while the higher floors have a rectangular plan. The steel superstructure is supported on a rigid concrete base, which is isolated from the ground by an isolation layer, as shown in Fig. 3(a). The superstructure consists of linear beam, column and bracing elements and rigid slabs. Below the base, the isolation layer is introduced for seismic mitigation. The superstructure is modeled as a three-dimensional linear elastic system with lateral-torsional behavior. The superstructure damping ratio is assumed to be 5%.

In this study, linear elastomeric bearings with low damping are considered as a base isolation system as shown in Fig. 4. The linear elastomeric isolation system consists of 92 low damping elastomeric bearings, and the fundamental period and the damping ratio of the system are $T_b = 3$ sec and 3%, respectively. More detailed information on the structural model can be found in Narasimhan, *et al.* (2006) and Nagarajaiah and Narasimhan (2006).

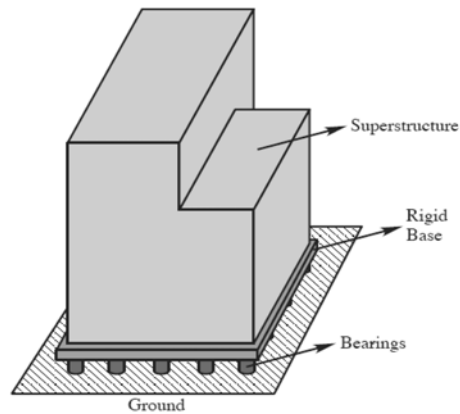


Fig. 3 A representative figure of the benchmark structure (Erkus and Johnson 2006)

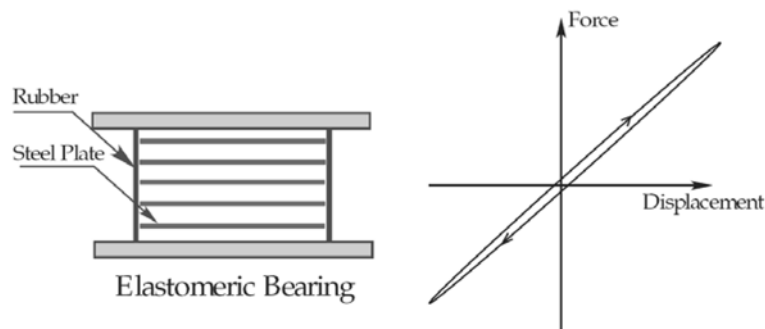


Fig. 4 Schematic of low damping elastomeric bearing and its force-displacement characteristics (Narasimhan, *et al.* 2006)

3.1.2. MR damper and its location

In this study, an MR damper is used as a basic supplemental control device for the base isolated building structure. The MR damper has a maximum force level of approximately ± 1000 kN, and the maximum command voltage is 10 Volts. Fig. 5 represents the phenomenological model of MR dampers based on the Bouc-Wen hysteretic model in parallel with a dashpot. All the parameters of the MR damper used in the study are described in the sample control design paper (Tan and Agrawal 2005).

The total of 16 supplemental active/semiactive control devices (i.e. actuators/MR dampers) are placed at the isolation level. Eight dampers are located in the X-direction and the other eight are in the Y-direction. Fig. 6(a) shows the elevation view with control devices and how to install the supplemental control devices. In Fig. 6(b), large circles represent supplemental control device locations, while small circles mean elastomeric bearing locations.

3.1.3. Earthquake records

The earthquakes used in this study are Newhall, Sylmar, El Centro, Rinaldi, Kobe, Jiji and Erzinkan earthquake records. The fault-normal (FN) and fault-parallel (FP) components of each earthquake record are considered. All the excitations are used at the full intensity for the evaluation of the performance indices. Fig. 7 shows time histories of these earthquake records.

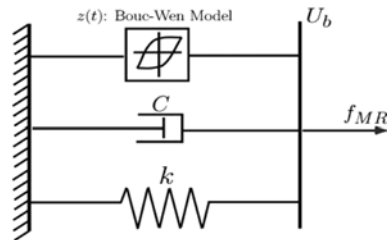
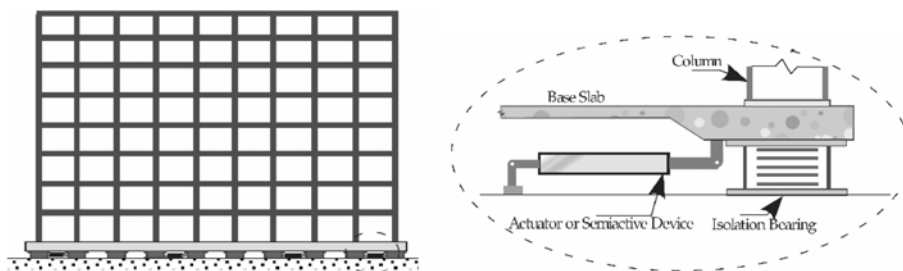
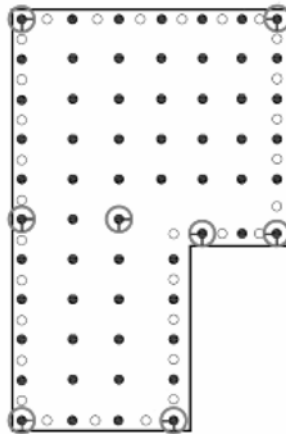


Fig. 5 Dynamic model of MR damper (Nagarajaiah and Narasimhan 2006)



(a) Elevation view with control devices



(b) Control device locations

Fig. 6 Configurations of supplemental control devices (Narasimhan, *et al.* 2006)

3.1.4. Evaluation criteria

To systematically evaluate the control performance of each control system, the nine evaluation criteria have been defined in the benchmark problem statements (Narasimhan, *et al.* 2006). First, the maximum responses (base shear (isolation-level) (J_1), structure shear (at first story level) (J_2), base displacement (or isolator deformation) (J_3), inter-story drift (J_4), and absolute floor acceleration (J_5)) are evaluated. From here, each index is normalized by the corresponding response in the uncontrolled structure. The peak control force generated by all control devices normalized by the peak base shear in the controlled structure (J_6) is also considered. Next, two RMS responses (base displacement (J_7), absolute floor acceleration (J_8)) are considered to

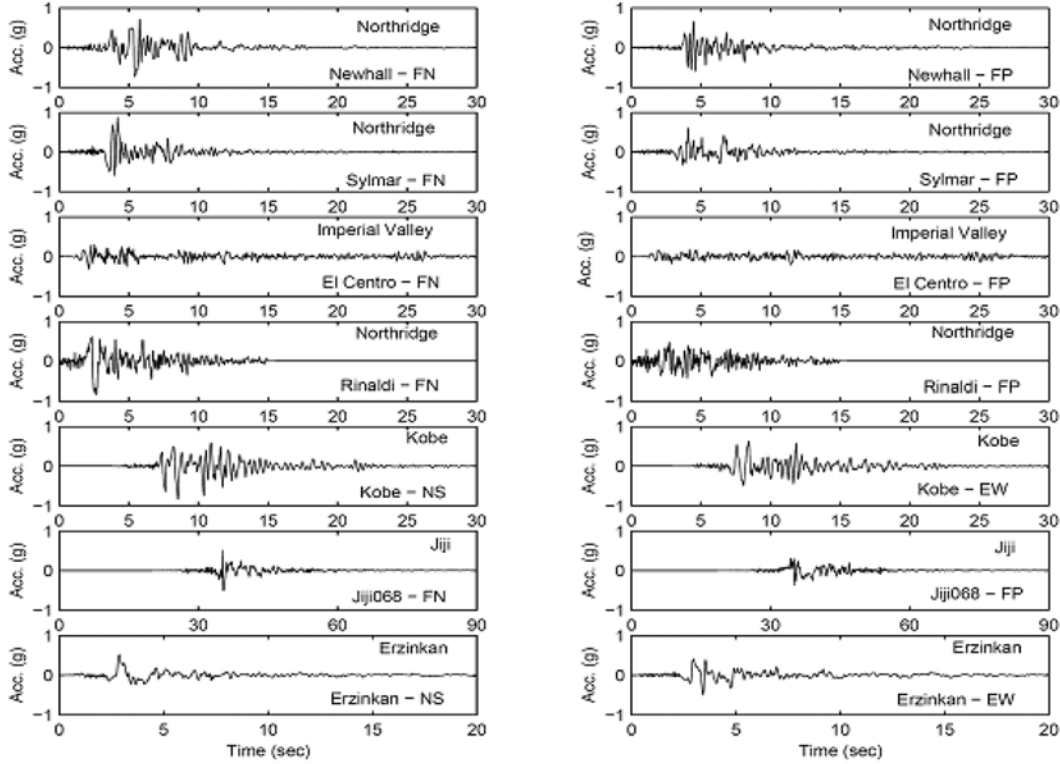


Fig. 7 Time-histories of earthquake records (Narasimhan, *et al.* 2006)

evaluate the average responses of the building. Finally, the dissipated total energy by the vibration control system (J_9) is evaluated.

3.1.5. Control systems compared

In this case, the conventional semiactive control system using MR dampers is considered to compare its control performance with that of the smart passive control system. In the semiactive system, the input voltage to an MR damper, u , is varied with command signal calculated by the well known clipped optimal control algorithm as follows:

$$u = V_{\max} H(\{f_c - f_{MR}\}f_{MR}) \tag{2}$$

where V_{\max} is the maximum voltage (Volt), H is the heaviside function, f_c is the optimal control force calculated from LQG algorithm (kN) and is the force that is generated by the f_{MR} damper (kN). For better performance, the control signal generated by the digital controller is passed through a low-pass filter before it is commanded to the device. The filter is given by

$$\dot{v} = -\zeta v + \zeta u \tag{3}$$

where the filter parameter $\zeta = 10$ rad/s. The force generated by the damper is a function of the voltage supplied. The damping force of the damper is obtained as

$$f_{MR} = (\alpha z)f(v) + C\dot{U}_b + kU_b \quad (4)$$

where $\alpha(v) = \alpha_a + \alpha_b v$, $C(v) = C_a + C_b v$, $f(v)$ is a function of the voltage v , supplied to the MR damper. The hysteresis variable z is governed by

$$Y_i \dot{z}_i + \gamma |\dot{U}_{bi}| z_i |z_i| + \beta U_{bi} z_i^2 - \dot{U}_{bi} = 0 \quad (5)$$

where U_b is the displacement experienced by the MR damper (m), and Y_i is the yield displacement of the hysteretic element (m), γ , β , α_a , α_b , C_a , and, C_b are constants.

In the smart passive control system, on the other hand, the electromotive force ε induced from an EMI part can be considered as the command voltage input to an MR fluid damper u (i.e. $u = \varepsilon$) instead of Eq. (2) in the semiactive control system.

3.1.6. Numerical simulation results

In this section, the numerical simulation results of the smart passive control system are compared with those of the conventional MR damper-based semiactive control system. First, a series of numerical simulations in the smart passive case are carried out with gradually increasing the gain of the EMI part (i.e. K_{emf}) as in Eq. (1) to obtain the appropriate value of K_{emf} . Figs. 8(a) and 8(b) show the average and maximum values of the evaluation criteria in the smart passive case for all the seven earthquakes, respectively. Also, Fig. 9 shows the mean values of the summation of all the evaluation criteria except the peak force and the total absorbed energy (i.e. from J_1 to J_9 except J_6 and J_9). As seen from Fig. 9, the minimum mean value is found at $K_{emf} = 5.0$. Hence, the smart passive system with $K_{emf} = 5.0$ is considered for comparison of the performance.

The results of evaluation criteria for the semiactive control system and the smart passive control system are presented in Tables 1 and 2, respectively. Table 1 shows the performance of the semiactive control system in the cases of all the seven earthquakes as well as average and maximum values. As seen from the table, the overall performance of the semiactive control system is good, but some evaluation criteria in some earthquake cases are increased compared to the uncontrolled case (e.g. $J_5 = 1.6311$ in the Kobe earthquake case). Table 2 shows the performance of the smart passive control system. As seen from the table, its overall performance is comparable to that of the semiactive case. The number of the evaluation criteria with more than 1.0 in the smart passive system is smaller than that in the semiactive case (i.e. 7 vs. 15). Moreover, the maximum values in the proposed case are smaller than those in the semiactive case as well. This clearly

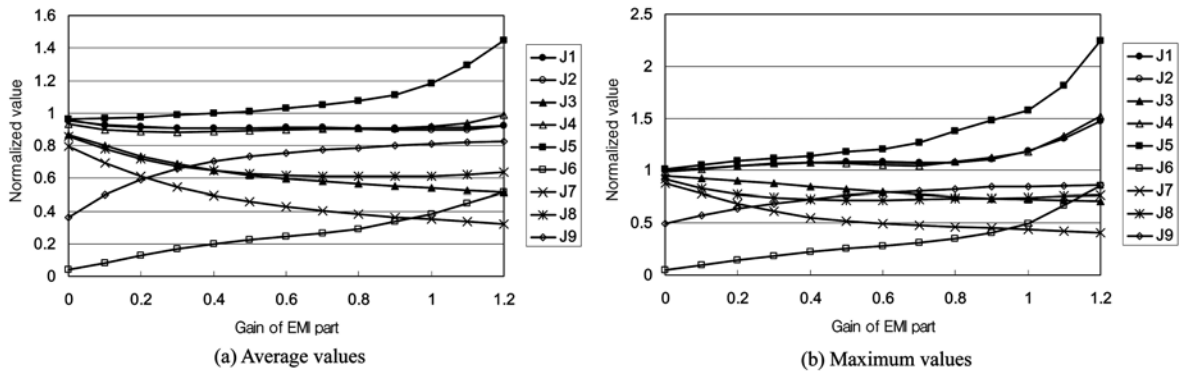


Fig. 8 Evaluation criteria according to variation of K_{emf}

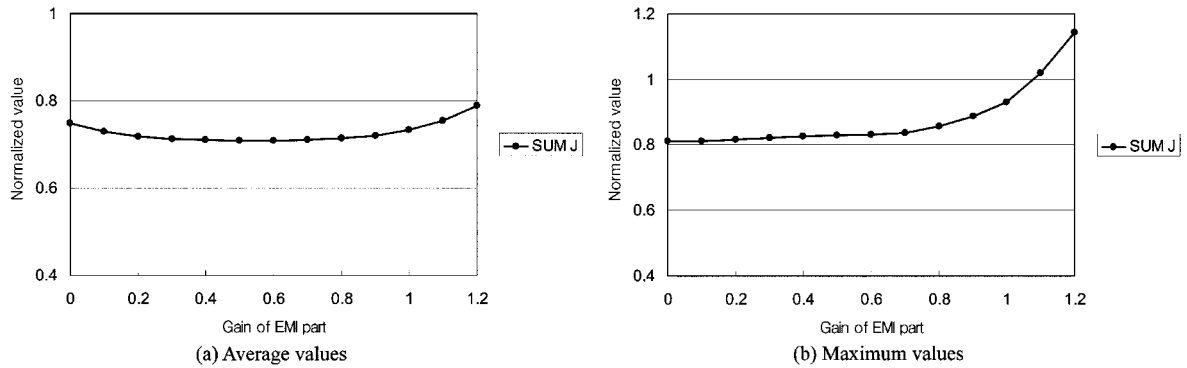


Fig. 9 Summation of evaluation criteria according to variation of K_{emf}

Table 1 Numerical simulation results of the semiactive control system

Criterion	Newhall	Sylmar	El Centro	Rinaldi	Kobe	Jiji	Erinkan	Aver.	Max.
J_1 (Peak Base Shear)	0.9709	0.9007	1.2519	1.0461	1.0438	0.8366	0.9285	0.9969	1.2519
J_2 (Peak Str. Shear)	1.0216	0.9138	1.2325	1.0227	1.0317	0.8413	0.9314	0.9993	1.2325
J_3 (Peak Isolator Deformation)	0.5594	0.7304	0.5418	0.5965	0.5185	0.6513	0.4656	0.5805	0.7304
J_4 (Peak I.S Drift)	1.0430	0.8656	1.2611	0.963	0.9939	0.857	0.8634	0.9781	1.2611
J_5 (Peak Absolute Acceleration)	1.4913	1.1593	1.6121	1.0113	1.6311	0.8737	1.2329	1.2874	1.6311
J_6 (Peak Force)	0.3014	0.2389	0.3814	0.2677	0.2836	0.1687	0.2533	0.2707	0.3814
J_7 (RMS Displacement)	0.3325	0.4503	0.4145	0.3787	0.2596	0.4598	0.3362	0.3759	0.4598
J_8 (RMS Acceleration)	0.8937	0.7369	0.7597	0.7141	0.733	0.7184	0.6261	0.7403	0.8937
J_9 (Total Absorbed Energy)	0.7946	0.8082	0.6494	0.7738	0.7308	0.6438	0.8018	0.7432	0.8082

Table 2 Numerical simulation results of the smart passive control system ($K_{emf} = 0.5$)

Criterion	Newhall	Sylmar	El Centro	Rinaldi	Kobe	Jiji	Erinkan	Aver.	Max.
J_1 (Peak Base Shear)	0.92060	0.8802	0.9188	1.0815	0.8458	0.8331	0.8746	0.9086	1.0815
J_2 (Peak Str. Shear)	0.9281	0.8931	0.8786	1.0815	0.8226	0.8376	0.8991	0.9058	1.0815
J_3 (Peak Isolator Deformation)	0.5966	0.8195	0.4622	0.7413	0.4651	0.7060	0.5380	0.6184	0.8195
J_4 (Peak I.S Drift)	0.9685	0.8680	0.7783	1.0639	0.8833	0.8520	0.8164	0.8901	1.0639
J_5 (Peak Absolute Acceleration)	1.0457	1.0734	0.9016	1.1042	1.1747	0.8644	0.9030	1.0098	1.1747
J_6 (Peak Force)	0.2561	0.2222	0.1005	0.2242	0.2258	0.1599	0.2365	0.2232	0.2561
J_7 (RMS Displacement)	0.3974	0.5139	0.6491	0.5022	0.4015	0.4986	0.5018	0.4579	0.5139
J_8 (RMS Acceleration)	0.7188	0.6981	0.6869	0.6245	0.5746	0.6734	0.5864	0.6293	0.7188
J_9 (Total Absorbed Energy)	0.7610	0.7560	0.5335	0.7496	0.7507	0.6028	0.7521	0.7328	0.7610

demonstrates that the robustness or adaptability of the smart passive system to the ground excitation could be better than that of the semiactive control system.

Fig. 10 shows the performance comparison between the semiactive control system and the smart passive control system. As shown in the figure, the control performance of the smart passive control system is slightly better than that of the semiactive control algorithm. Moreover, all the criteria in the smart passive system are less than or at least similar to 1.0 while some in the semiactive system are

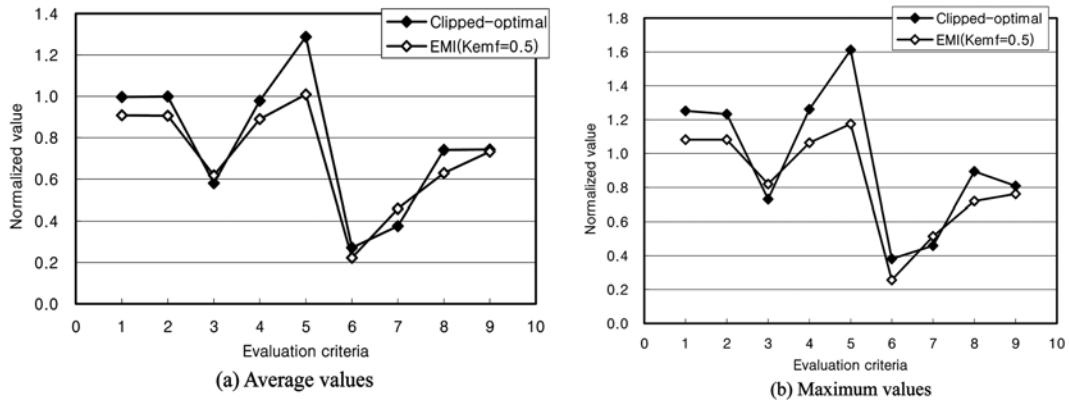


Fig. 10 Comparison of control performance of two control systems

slightly larger than 1.0. Note that the sample controller provided by Nagarajaiah and Narasimha (2006) is used in the semiactive control case, which is not meant to be competitive and hence, further reductions are possible even with better control algorithms. It is verified from the numerical simulation that the smart passive system could be able to effectively reduce the structural responses by itself without any feedback control system including sensors, a controller and an external power source in the case of base isolated building structures.

The time history responses of the smart passive control system are compared to those of the uncontrolled case for the El Centro earthquake as shown in Fig. 11. According to the figure, in the semiactive system, the peak value of the isolator deformation is significantly reduced, whereas the floor acceleration is slightly increased. On the other hand, the smart passive system can reduce the isolator deformation without increasing the floor acceleration as shown in Fig. 11.

3.2. Example 2: base isolated highway bridge structure

3.2.1. Structural model

The highway bridge structure considered in this study is based on the newly constructed 91/5 highway over-crossing in southern California, USA as shown in Fig. 12. It is a continuous two-span, cast-in-place prestressed concrete box-girder bridge. The bridge has two spans, each of 58.52 m long spanning a four-lane highway and has two abutments skewed. The width of the deck is 12.95 m and the columns are approximately 6.9 m high. The elevation and plan views of the bridge, and the idealized model of the bridge are illustrated in Fig. 12(a) and (b), respectively. There are total eight bearings between bridge deck and abutments to isolate the bridge superstructure at both abutment-ends. The bearings are idealized by bi-directional bilinear plasticity model. Detailed information on the bridge structure and its finite element model can be found in the problem definition paper (Agrawal, *et al.* 2005).

3.2.2. MR dampers and its location

An MR damper is used as a basic supplemental control device. The MR damper has a maximum force level of approximately ± 1000 kN, and the maximum command voltage is 10 Volts. Fig. 13 represents the phenomenological model of MR dampers based on the Bouc-Wen hysteretic model in

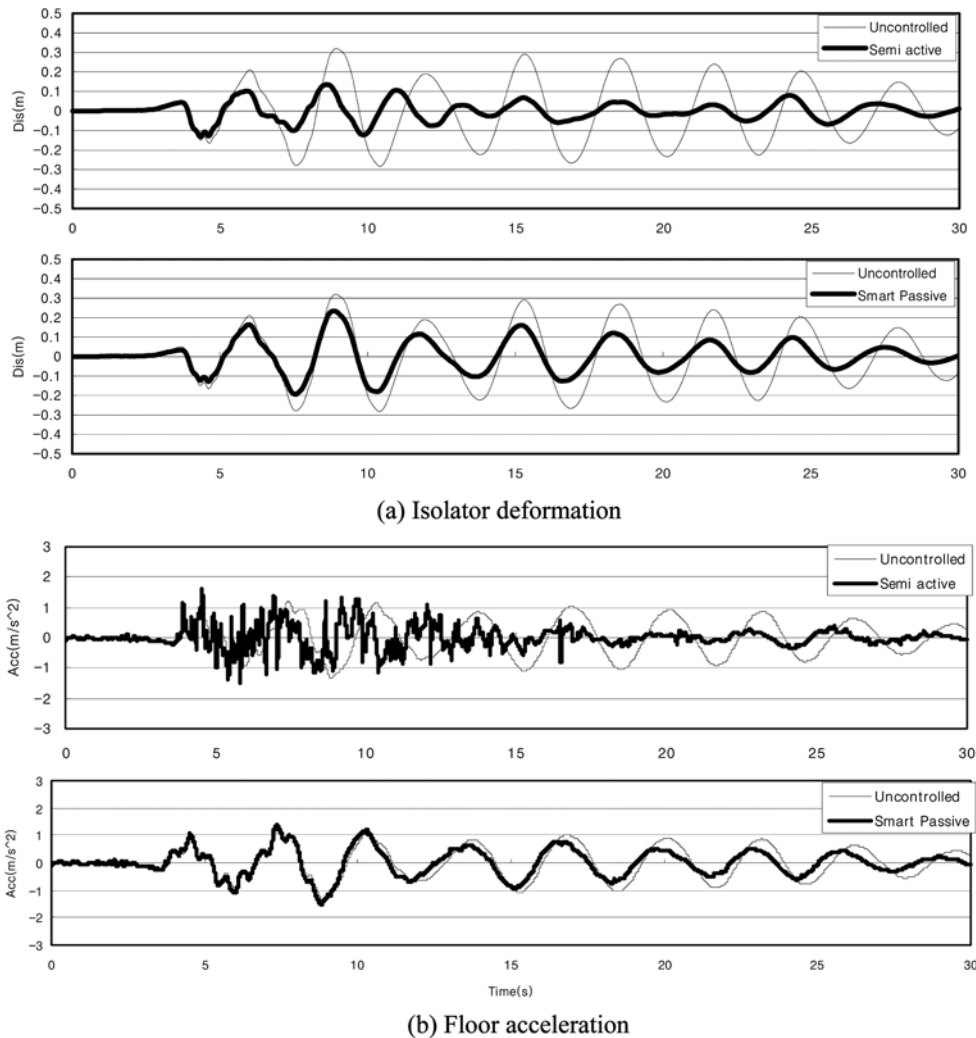


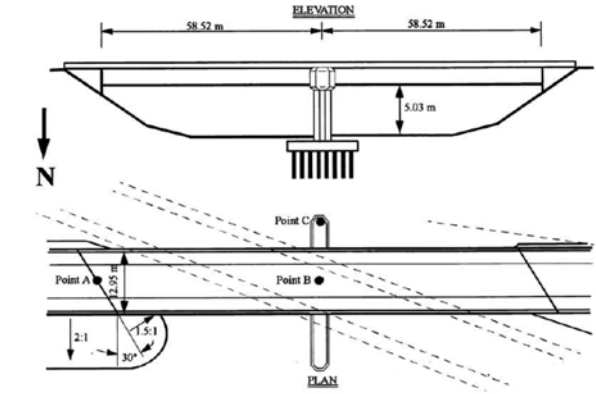
Fig. 11 Time history responses under the El Centro earthquake

parallel with a dashpot. All the parameters of the MR damper used in the study are described in the sample control design paper (Tan and Agrawal 2005).

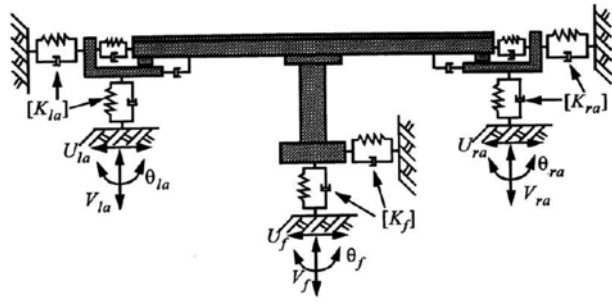
Control devices such as MR dampers are placed orthogonally between the deck-ends and both abutments of the bridge. There are total of 16 devices, 8 at each end of bridge, are employed to reduce the earthquake-induced vibrations of the bridge as shown in Fig. 14. In a conventional semiactive control case, the sensors should be also located as demonstrated in the below figure.

3.2.3. Earthquake ground motions

Six earthquake ground motions are considered in this study. These earthquakes are: North Palm Springs (1986), TCU084 component of Chi-Chi earthquake, Taiwan (1999), El Centro component of 1940 Imperial Valley earthquake, Rinaldi component of Northridge (1994) earthquake, Bolu component of

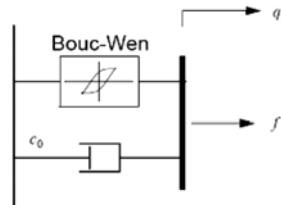


(a) The elevation and plan views of the bridge



(b) The idealized model of the bridge

Fig. 12 Base isolated highway bridge (Agrawal, *et al.* 2005)



(a) Dynamic model of MR damper

Fig. 13 MR damper (Tan and Agrawal 2005)

Duzce, Turkey (1999) earthquake and Nishi-Akashi component of Kobe (1995) earthquakes. Fig. 15 shows time histories of these earthquakes.

3.2.4. Evaluation criteria

To systematically evaluate the control performance of different control systems, a set of 16 normalized evaluation criteria have been developed as follows (Agrawal, *et al.* 2005): peak base shear force (J_1), peak overturning moment (J_2), peak displacement at midspan (J_3), peak acceleration at midspan (J_4), peak deformation of bearings (J_5), peak curvature at bent column (J_6), peak dissipated energy of curvature at bent column (J_7), the number of plastic connections (J_8), normed base shear force (J_9), normed overturning moment (J_{10}), normed displacement at the midspan (J_{11}), normed acceleration at midspan (J_{12}), normed deformation of bearings (J_{13}), normed curvature at bent column (J_{14}), peak control force (J_{15}), and peak

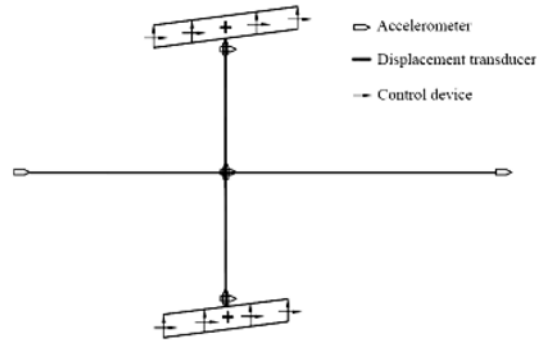


Fig. 14 Locations and directions of control devices (Tan and Agrawal 2005)

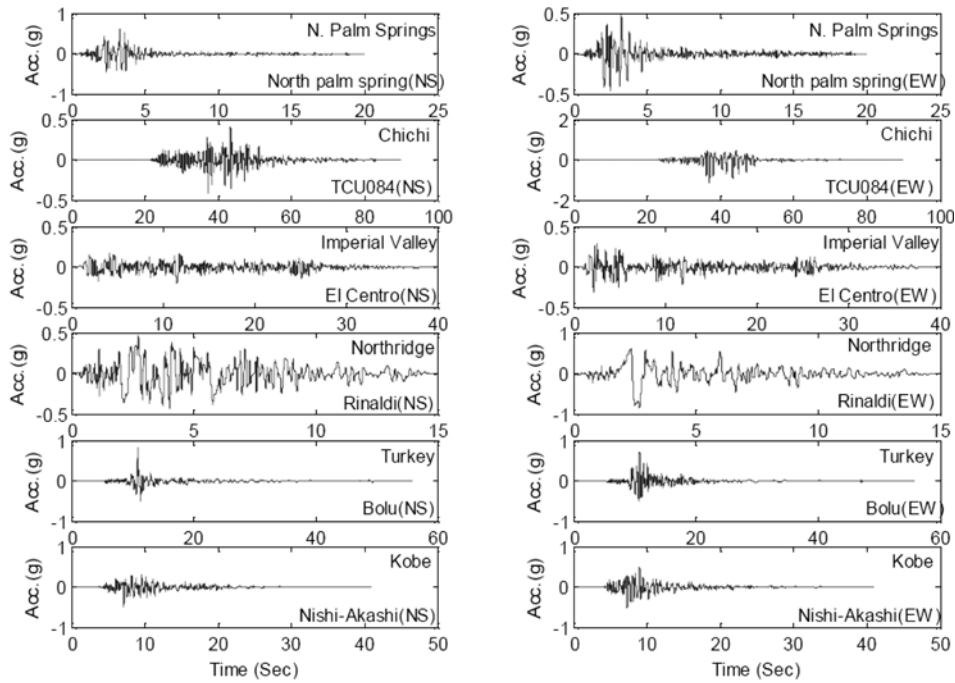


Fig. 15 Earthquake ground motions (Agrawal, *et al.* 2005)

stroke of the control devices (J_{16}). Detailed information on the evaluation criteria can be found in Agrawal, *et al.* (2005).

3.2.5. Control systems compared

In this case, the performance of the smart passive control system is compared with that of the conventional semiactive control system using MR dampers. In the semiactive system, the input voltage to an MR damper, u , is calculated as in Eq. (2).

The control force of the MR damper is given by

$$f_{MR} = c_0 \dot{x} + \alpha z \tag{6}$$

where c_0 is the damping coefficient of the damper and the evolutionary variable z is governed by

$$\dot{z} = -\gamma|\dot{x}|z|z|^{n-1} - \beta\dot{x}|z|^n + A\dot{x} \tag{7}$$

The parameters γ , n , β , and A are controlling the linearity in the unloading and the smoothness of the transition from the pre-yield to the post-yield region. The functional dependence of the device parameters on the command voltage u is expressed as

$$\begin{aligned} \alpha &= \alpha(u) = \alpha_a + \alpha_b u \\ c_0 &= c_0(u) = c_{0a} + c_{0b} u \end{aligned} \tag{8}$$

where coefficients α_a , α_b , c_{0a} , and c_{0b} are determined by linear regression of experimental data.

In the smart passive control system, on the other hand, the electromotive force ε induced from an EMI part can be considered as the command voltage input to an MR fluid damper u (i.e. $u = \varepsilon$) instead of Eq. (2) in the semiactive control system.

3.2.6. Numerical simulation results

The numerical simulation results of the smart passive control system are compared with those of the conventional MR damper-based semiactive control system employing the widely used clipped-optimal control algorithm (Dyke and Spencer 1996, Spencer, *et al.* 1997).

Fig. 16(a) and Fig. 16(b) shows the average and maximum values of the evaluation criteria in the smart passive control system for all the six earthquakes as the gain of the EMI part (K_{emf}) increases, respectively. Fig. 17 represents the summation of all the evaluation criteria. According to the figure, its minimum value is found at $K_{emf} = 70$ as regard to the average values. On the other hand, the case of $K_{emf} = 5$

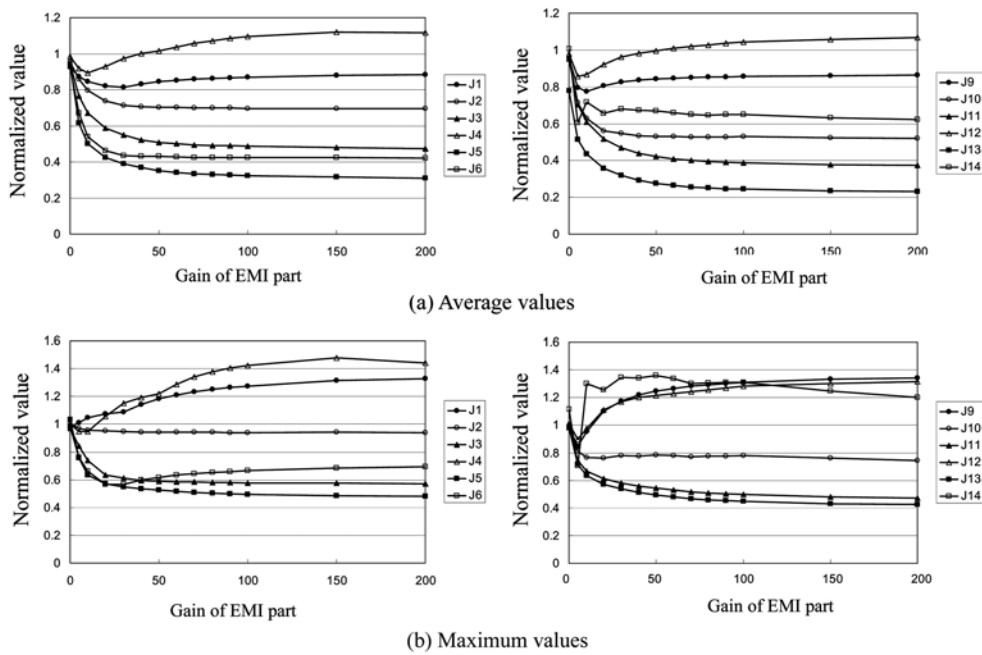


Fig. 16 Maximum results in the smart passive system for all the earthquakes

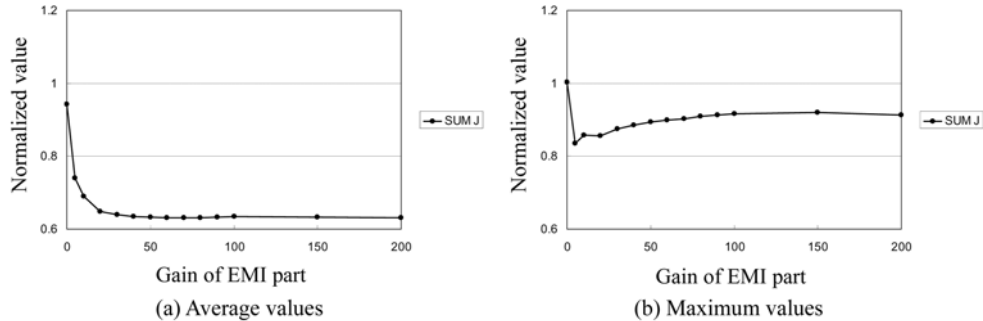


Fig. 17 Summation of evaluation criteria according to variation of K_{emf}

shows the best performance from the viewpoint of the maximum values as shown in Fig. 17(b).

The results of evaluation criteria for the semiactive control system and the smart passive control system are presented in Tables 3 to 5. Table 3 shows the performance of the semiactive control system in the cases of all the seven earthquakes as well as average and maximum values. As seen from the table, the overall performance of the semiactive control system is good. Table 4 represents the performance of the smart passive control system with $K_{emf} = 5$. It is demonstrated from the table that its overall performance is comparable to that of the semiactive case. Table 5 shows the performance of the smart passive control system with $K_{emf} = 70$. In this case, some criteria are much less than 1.0, while some are much larger than 1.0. That is, the smart passive system with $K_{emf} = 70$ does not have the robustness to the ground excitations.

The results of the smart passive control system are compared with those of the semiactive control system employing the clipped-optimal control algorithm as demonstrated in Fig. 17. As shown in the figure, the

Table 3 Numerical simulation results of the semiactive control system

Criterion	N. Palm Springs	Chichi	El Centro	Northridge	Turkey	Kobe	Aver.	Max.
J_1 (Max Base Shear)	0.9619	0.8416	0.7792	0.8857	0.9039	0.8174	0.8650	0.9619
J_2 (Max Base Moment)	0.7476	0.9781	0.7081	0.9790	0.9788	0.6642	0.8426	0.9790
J_3 (Max Midspan Displacement)	0.8024	0.7852	0.7753	0.8570	0.7166	0.6632	0.7666	0.8570
J_4 (Max Midspan Acceleration)	0.9814	0.8757	0.8956	0.8993	0.8003	0.9858	0.9064	0.9814
J_5 (Max Abutment Displacement)	0.8121	0.7647	0.5662	0.8532	0.6744	0.5097	0.6967	0.8532
J_6 (Max Ductility)	0.7476	0.6959	0.7081	0.8276	0.3717	0.6642	0.6692	0.8276
J_7 (Max Dissipated Energy)	0	0.4682	0	0.5674	0.2364	0	0.2120	0.5674
J_8 (Max Plastic Connections)	0	0.6667	0	1.0000	0.3333	0	0.3333	1.0000
J_9 (Norm Base Shear)	0.7792	0.8457	0.5970	0.8288	0.8402	0.6909	0.7636	0.8457
J_{10} (Norm Base Moment)	0.6622	0.7984	0.5594	0.8378	0.5019	0.6560	0.6693	0.8378
J_{11} (Norm Midspan Displacement)	0.6825	0.7532	0.5797	0.7772	0.5732	0.6743	0.6734	0.7772
J_{12} (Norm Midspan Acceleration)	0.7894	0.8074	0.6895	0.8178	0.8087	0.8376	0.7917	0.8376
J_{13} (Norm Abutment Displacement)	0.4543	0.7460	0.3929	0.7744	0.4045	0.3679	0.5233	0.7744
J_{14} (Norm Ductility)	0.6622	0.6927	0.5594	0.7713	0.2204	0.6560	0.5937	0.7713
J_{15} (Max Control Force)	0.0109	0.0227	0.0084	0.0226	0.0157	0.0096	0.0150	0.0227
J_{16} (Max Device Stroke)	0.7817	0.7322	0.5207	0.7772	0.6685	0.5025	0.6638	0.7817

Table 4 Numerical simulation results of the smart passive control system ($K_{emf} = 5$)

Criterion	N. Palm Springs	Chichi	El Centro	Northridge	Turkey	Kobe	Aver.	Max.
J ₁ (Max Base Shear)	1.0102	0.7460	0.8317	0.7818	0.8713	0.8630	0.8735	1.0102
J ₂ (Max Base Moment)	0.7049	0.9662	0.7609	0.9651	0.9698	0.6810	0.8597	0.9698
J ₃ (Max Midspan Displacement)	0.7295	0.7787	0.8441	0.7948	0.6925	0.6792	0.7661	0.8441
J ₄ (Max Midspan Acceleration)	0.8718	0.9479	0.9088	0.9018	0.9095	0.9287	0.9166	0.9479
J ₅ (Max Abutment Displacement)	0.6012	0.7278	0.4760	0.7569	0.6526	0.3501	0.6174	0.7569
J ₆ (Max Ductility)	0.7049	0.6553	0.7609	0.7036	0.4219	0.6810	0.6698	0.7609
J ₇ (Max Dissipated Energy)	0	0.4508	0	0.4685	0.1913	0	0.2256	0.4685
J ₈ (Max Plastic Connections)	0	0.6667	0	1.0000	0.3333	0	0.4286	1.0000
J ₉ (Norm Base Shear)	0.8362	0.8458	0.6587	0.7930	0.8370	0.7496	0.7952	0.8458
J ₁₀ (Norm Base Moment)	0.7089	0.7977	0.6169	0.8134	0.5502	0.7009	0.7145	0.8134
J ₁₁ (Norm Midspan Displacement)	0.7369	0.7428	0.6380	0.7406	0.5837	0.7312	0.7023	0.7428
J ₁₂ (Norm Midspan Acceleration)	0.8148	0.8719	0.7715	0.8589	0.8821	0.8958	0.8558	0.8958
J ₁₃ (Norm Abutment Displacement)	0.3560	0.7182	0.4080	0.7145	0.3960	0.2813	0.5132	0.7182
J ₁₄ (Norm Ductility)	0.7089	0.5284	0.6169	0.6432	0.3307	0.7009	0.6054	0.7089
J ₁₅ (Max Control Force)	0.0084	0.0198	0.0056	0.0176	0.0130	0.0071	0.0130	0.0198
J ₁₆ (Max Device Stroke)	0.5787	0.6968	0.4377	0.6894	0.6469	0.3542	0.5845	0.6968

Table 5 Numerical simulation results of the smart passive control system ($K_{emf} = 70$)

Criterion	N. Palm Springs	Chichi	El Centro	Northridge	Turkey	Kobe	Aver.	Max.
J ₁ (Max Base Shear)	1.2338	0.5745	0.6006	0.6669	0.7103	0.9896	0.8585	1.2338
J ₂ (Max Base Moment)	0.6438	0.9408	0.3384	0.9400	0.5742	0.5263	0.7006	0.9408
J ₃ (Max Midspan Displacement)	0.4477	0.5525	0.3472	0.5666	0.3892	0.5829	0.4956	0.5829
J ₄ (Max Midspan Acceleration)	1.3410	0.8553	0.9996	0.8110	0.8460	1.2011	1.0565	1.3410
J ₅ (Max Abutment Displacement)	0.1855	0.4999	0.1132	0.5082	0.3171	0.2063	0.3341	0.5082
J ₆ (Max Ductility)	0.6438	0.3440	0.3384	0.3588	0.1265	0.5263	0.4259	0.6438
J ₇ (Max Dissipated Energy)	0	0.0243	0	0.1130	0	0	0.0358	0.1130
J ₈ (Max Plastic Connections)	0	0.3333	0	0.5000	0	0	0.1905	0.5000
J ₉ (Norm Base Shear)	1.2808	0.5163	0.5752	0.5776	0.8536	0.8686	0.8504	1.2808
J ₁₀ (Norm Base Moment)	0.6339	0.5296	0.2908	0.7705	0.2366	0.4570	0.5270	0.7705
J ₁₁ (Norm Midspan Displacement)	0.4278	0.3884	0.2658	0.5171	0.2742	0.4142	0.4007	0.5171
J ₁₂ (Norm Midspan Acceleration)	1.2056	0.6553	0.8254	0.8039	1.1534	1.2430	1.0185	1.2430
J ₁₃ (Norm Abutment Displacement)	0.1078	0.3479	0.1161	0.4687	0.1646	0.1177	0.2559	0.4687
J ₁₄ (Norm Ductility)	0.6339	0.5337	0.2908	1.3020	0.0228	0.4570	0.6489	1.3020
J ₁₅ (Max Control Force)	0.0243	0.0256	0.0213	0.0254	0.0249	0.0247	0.0245	0.0256
J ₁₆ (Max Device Stroke)	0.1786	0.4786	0.1041	0.4629	0.3144	0.2034	0.3172	0.4786

control performance of the smart passive control system with $K_{emf} = 5$ is comparable to that of the semiactive control algorithm. On the other hand, the control performance of the smart passive control system with $K_{emf} = 70$ is not good compared to other control systems. Thus, it is noted that the smart passive system with the appropriate gain of the EMI part could be able to effectively reduce the structural responses by itself without any

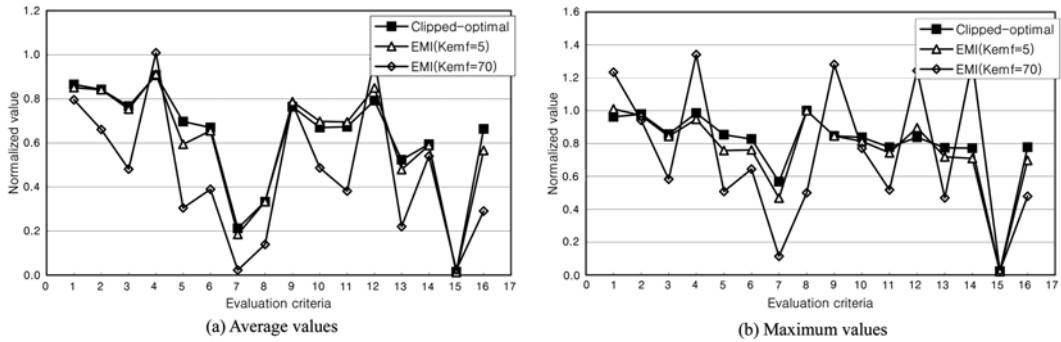


Fig. 18 Comparison of control performance of two control systems

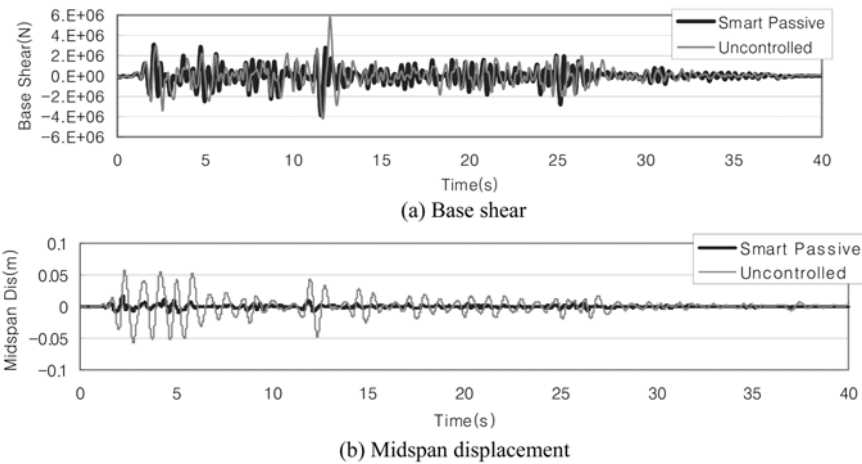


Fig. 19 Time history responses under El Centro earthquake

feedback control system including sensors, a controller and an external power source.

The time history responses of the smart passive control system are compared to those of the uncontrolled case for the El Centro earthquake as shown in Fig. 19. According to the figure, the peak values of the base shear force and the displacement of midspan are reduced by about 30% and 70%, respectively, owing to the adaptive passive system. It can be seen that the adaptive passive system achieves the significant control performance with respect to the base shear as well as the midspan displacement.

4. Conclusions

The effectiveness of the smart passive control system employing a magnetorheological (MR) damper and an electromagnetic induction (EMI) part for seismic protection of base isolated structures such as buildings and highway bridges is numerically investigated. An EMI part consists of a permanent magnet and a coil, which changes the kinetic energy of the deformation of an MR damper into the electric energy (i.e., the induced current) according to the Faraday’s law of electromagnetic induction. In the smart passive control system, the damping characteristics of the MR damper are varied with the current

input generated from the EMI part. Hence, the smart passive control system does not need any control system consisting of sensors, a controller and an external power source.

To verify the efficacy of the smart passive control system, a series of numerical simulations are carried out by considering the benchmark base isolated structure control problems developed by the ASCE structural control committee. The benchmark structures considered are the eight-story frame building with steel-braces and a continuous two-span concrete box-girder bridge, respectively. The numerical simulation results show that the smart passive control system has the comparable control performance to the conventional MR damper-based semiactive control system. Because of its simplicity and cost-effectiveness as well as the comparable performance, the smart passive control system could be beneficial in reducing seismic responses of the base isolated structures. Therefore, the smart passive control system could be considered as one of the promising control devices for seismic protection of seismically excited base isolated structures.

Acknowledgements

The authors gratefully acknowledge the support of this research by the Smart Infra-Structure Technology Center (SISTeC) supported by the Korea Science Foundation and the Ministry of Science and Technology in Korea, and the Construction Core Technology Research and Development Project (Grant No.: C105A1000021-06A0300-01910) supported by the Ministry of Construction and Transportation in Korea.

References

- Agrawal, A. K., Tan, P., Nagarajaiah, S. and Zhang, J. (2005), "Benchmark structural control problem for a seismically excited highway bridge, part I: problem definition", <http://www-ce.engr.cuny.edu/People/Agrawal>.
- Battaini, M., Casciati, F. and Faravelli, L. (1998), "Fuzzy control of structural vibration. an active mass system driven by a fuzzy controller", *Earthq. Eng. Struct. Dyn.*, **27**, 1267-1276.
- Cho, S. W., Jung, H. J. and Lee, I. W. (2005), "Smart passive system based on magnetorheological damper", *Smart Mater. Struct.*, **14**, 707-714.
- Choi, K. M., Cho, S. W., Jung, H. J. and Lee, I. W. (2004), "Semiactive fuzzy control for seismic response reduction using MR dampers", *Earthq. Eng. Struct. Dyn.*, **33**(6), 723-736.
- Dyke, S. J., Spencer Jr., B. F., Sain, M. K. and Carlson, J. D. (1996), "Modeling and control of magnetorheological dampers for seismic response reduction", *Smart Mater. Struct.*, **5**, 565-575.
- Dyke, S. J. and Spencer Jr., B. F. (1996), "Seismic response control using multiple MR dampers", *2nd International Workshop on Structural Control*. Hong Kong, 163-173.
- Dyke, S. J., Spencer Jr., B. F., Sain, M. K. and Carlson, J. D. (1998), "An experimental study of MR dampers for seismic protection", *Smart Mater. Struct.*, **7**, 693-703.
- Erkus, B. and Johnson, E. A. (2006), "Smart base-isolated benchmark building Part III: a sample controller for bilinear isolation", *J. Struct. Control Health Monit.*, **13**, 605-625.
- Inaudi, J. A. (1997), "Modulated homogeneous friction: a semi-active damping strategy", *Earthq. Eng. Struct. Dyn.*, **26**(3), 361-376.
- Jansen, L. M. and Dyke, S. J. (2000), "Semi-active control strategies for MR dampers: a comparative study", *J. Eng. Mech.*, ASCE, **126**, 795-803.
- Jung, H. J., Choi, K. M., Spencer Jr., B. F. and Lee, I. W. (2006), "Application of some semi-active control algorithms to a smart base-isolated building employing MR dampers", *J. Struct. Control Health Monit.*, 693-704.
- Lee, H. J., Yang, G., Jung, H. J., Spencer Jr., B. F. and Lee, I. W. (2006), "Semi-active neurocontrol of a base-isolated benchmark structure", *J. Struct. Control Health Monit.*, **13**, 682-692.

- Kamath, G. M. and Wereley, N. M. (1997), "A nonlinear viscoelastic-plastic model for electrorheological fluids", *Smart Mater. Struct.*, **6**, 351-359.
- Marshall, S. V. and Skitek, G. G. (1999), *Electromagnetic Concepts and Applications*, Englewood Cliffs, NJ: Prentice-Hall.
- McClamroch, N. H. and Gavin, H. P. (1995), "Closed loop structural control using electrorheological dampers," *Proceedings of the American Control Conference*, Seattle, Washington, 4173-4177.
- Miner, G. F. (1996), *Lines and Electromagnetic Fields for Engineers*, Oxford: Oxford University Press.
- Nagarajaiah, S. and Narasimhan, S. (2003), "Controllers for benchmark base isolated building with linear and friction isolation system," *Proceeding of the 16th Engineering Mechanics Conference*, ASCE, Univ. of Washington, Seattle, CD-ROM.
- Nagarajaiah, S. and Narasimhan, S. (2004), "Phase I: Controllers for benchmark base isolated building: Part I," *Proceeding of the 4th International Workshop on Structural Control and Health Monitoring*, Columbia Univ., New York, CD-ROM.
- Nagarajaiah, S. and Narasimhan, S. (2006), "Phase I smart base isolated benchmark building – sample controllers for linear isolation system: Part II", *J. Struct. Control and Health Monit.*, **13**, 589-604.
- Narasimhan, S., Nagarajaiah, S., Johnson, E. A. and Gavin, H. P. (2003), "Smart base isolated building benchmark problem", *Proceeding of the 16th Engineering Mechanics Conference*, ASCE, Univ. of Washington, Seattle, CD-ROM.
- Narasimhan, S., Nagarajaiah, S., Johnson, E. A. and Gavin, H. P. (2004), "Smart base isolated benchmark building part I: Problem definition", *Proceeding of the 4th International Workshop on Structural Control and Health Monitoring*, Columbia Univ., New York, CD-ROM.
- Narasimhan, S., Nagarajaiah, S., Johnson, E. A. and Gavin, H. P. (2006), "Smart base isolated benchmark building part I: Problem definition", *J. Struct. Control and Health Monit.*, **13**, 573-588.
- Ramallo, J. C., Johnson, E. A. and Spencer, B. F., Jr. (2002), "Smart base isolation systems", *J. Eng. Mech.*, ASCE, **128**, 1088-1099.
- Reitz, J. R., Milford, F. J. and Christy, R. W. (1993), *Foundations of Electromagnetic Theory*, Reading, MA: Addison-Wesley.
- Skinner, R. I., Robinson, W. H. and McVerry, G. H. (1993), *An Introduction to Base Isolation*, John Wiley & Sons Ltd., Chichester, England.
- Soong, T. T. and Constantinou. M. C. (Eds.) (1994), *Passive and Active Structural Vibration Control in Civil Engineering*, Springer-Verlag, Wien and New York.
- Spencer Jr., B. F., Dyke, S. J., Sain, M. F. and Carlson, J. D. (1997), "Phenomenological model of a magnetorheological damper", *J. Eng. Mech.*, ASCE, **123**, 230-238.
- Tan, P. and Agrawal, A. K. "Benchmark structural control problem for a seismically excited highway bridge, part II: sample control designs", <http://www-ce.engr.cuny.cuny.edu/People/Agrawal>, 2005.
- Yang, J. N., Wu, J. C., Reinhorn, A. M. and Riley, M. (1996), "Control of sliding-isolated buildings using sliding-mode control", *J. Struct. Eng.*, **122**, 179-186.
- Yoshida, O. and Dyke, S. J. (2004), "Seismic control of a nonlinear benchmark building using smart dampers", *J. Eng. Mech.*, **130**, 386-392.